Local Strain-Mediated Chemical Potential Control of Quantum Dot Self-Organization in Heteroepitaxy

Bin Yang,[1] Feng Liu,[2] and M. G. Lagally[1]

[1]*University of Wisconsin–Madison, Madison, Wisconsin 53706, USA*
[2]*University of Utah, Salt Lake City, Utah 84112, USA*
(Received 23 May 2003; published 15 January 2004)

From observations of self-assembly of Ge quantum dots directed by substrate morphology, we propose the concept of control of ordering in heteroepitaxy by a local strain-mediated surface chemical potential. Using quite simple lithography, we demonstrate directed quantum dot ordering. The strain part of the chemical potential is caused by the spatially nonuniform relaxation of the strained layer, which in our study is the Ge wetting layer, but, more generally, can be a deposited strained buffer layer. This model provides a consistent picture of prior literature.

In quantum dots (QDs), structures with dimensions small enough that their properties approach those of atoms, the spatial confinement of carriers leads to quantized energy levels, whose position and width depend strongly on the size of the QDs. QD electronic and optical properties can therefore be manipulated by controlling the dimensions of the QDs, making them promising building blocks for future nanoelectronic and optoelectronic devices [1–3]. A variety of techniques can be used to fabricate QDs. Among these, self-assembly via Stranski-Krastanov growth in heteroepitaxial systems [4–6] has attracted much interest (for reviews, see [7–9]), because of its compatibility with conventional wafer processing techniques. Because growth is stochastic, the size uniformity and spatial order of QDs required for many technological applications are not readily achievable.

Approaches that in some manner direct the growth and ordering of QDs have been explored to improve spatial ordering and size uniformity [10–17]. One is the use of nanopatterned substrates as templates [11–17]. QDs have been grown with very good spatial order and size uniformity on nanopatterned stripes and mesas [11,15]. There are both practical and fundamental difficulties with results so far. Practically, nanopatterning is difficult and time consuming, and thus negates many of the advantages of self-assembly. Furthermore, the physical mechanisms of ordering on these patterned substrates are not understood. It is not clear if nanomorphologies are required for the directed ordering.

In this Letter, we provide physical insights into directed ordering using substrate morphology, developing the concept of a locally varying strain-mediated surface chemical potential. We use simple conventional processing, rather than complex nanopatterning, to create templates. We show that even much coarser morphologies, when appropriately treated, produce very good ordering, implying nanomorphologies are not required for directed assembly. We propose a simple model to elucidate the

ordering of Ge QDs on stripes and mesas by introducing a strain-energy-dependent term, in addition to the common surface-energy term, into the chemical potential. We show that, while the surface energy always produces a minimum chemical potential at regions of negative surface curvature, the strain term can give rise to a local minimum chemical potential at regions of positive curvature. The competition between these two terms controls the preferred nucleation and growth of QDs. By tuning the relative strengths of these two contributions, it is possible to grow QDs selectively where desired.

We fabricate surface morphologies, in the micrometer range, on Si(001) via conventional lithography. We make crossed stripes with a 2 μm top width, which are etched to a depth of 2.5 μm. Their orientation does not influence the Ge QD alignment. Samples were chemically cleaned, outgassed in vacuum at 650 °C for several hours, and then rapidly heated to 1200 °C for several seconds at a time, while keeping the pressure lower than 3×10^{-9} Torr. Ge was deposited at 650 °C at a growth rate of 0.8 ML/min in an ultrahigh vacuum chemical vapor deposition system using disilane and digermane sources, to nominal coverages between 20 to 60 monolayers (ML).

It is well known that annealing modifies the topography of etched structures [18,19]. The topography evolves via mass transport controlled by the chemical-potential: atoms diffuse from regions of high chemical potential to regions of lower chemical potential. The evolution to a rounded topography can be described by a simple continuum model [18], which assumes a linear dependence of the surface chemical potential on surface curvature $\kappa(x, y)$ [20], i.e.,

$$\mu = \mu_0 + \Omega\gamma\kappa(x, y), \tag{1}$$

where μ_0 is the chemical potential for the flat surface, Ω is the atomic volume, and γ is the surface free energy per unit area. The second term represents the surface curvature contribution. In a curved surface, convex regions (positive curvature) have a higher chemical potential

than concave regions (negative curvature). Atoms diffuse from convex regions to concave regions.

We have simulated the morphological evolution of patterned structures (stripes and mesas) under high-temperature annealing, as shown in Figs. 1(a) and 1(b). With annealing, the originally flat top of patterned structures evolves into a smooth rounded shape. The shape evolution depends on the size of starting structures. For an annealing time that allows the top of an originally flat narrow stripe to evolve into a single ridge with a convex top, the top of a wide mesa evolves into a shape with a lower central region and convex humps at the sides [21]. Mass transport generally starts in a small region near the curvature extremes. Atoms diffuse from highly convex regions (mesa edges) not only down to the concave feet, but also inwards to the flat tops of the patterned structures, forming humps near the mesa edges. At bottoms of the patterned structures, atoms diffuse inward from flat regions to the concave regions (mesa feet), leaving dips behind. Continued annealing of a mesa structure drives the two convex humps toward the center, eventually merging into one ridge, and the dips at the foot of the mesa outward.

The simulated morphologies closely resemble those created in the experiments. Figure 2 shows atomic-force microscopy (AFM) images and line scans of a ridge and a stripe cross created after annealing an array of crossing stripes (a larger view is shown in Fig. 3). Figure 2 demonstrates Ge dome-type QDs growing with very good spatial and size control. Similar images have been shown, but using nanopatterned substrates [11,12,15].

This type of self-assembly extends uniformly over large distances. Figure 3 shows scanning electron microscope (SEM) images of self-assembled Ge QDs on a cross pattern of stripes. The stripes are 10 μm apart and originally had $\sim$2 μm wide flat tops. At the crosses of stripes, mesas with 3 μm wide square tops are formed, with vaulted edges in $\langle 100 \rangle$ directions, as shown in Fig. 2(b). Ge QDs grow along the ridges of stripes and the edges of stripe-cross mesas, with remarkable spatial order, forming a diamond shape of QDs at the stripe-cross mesas. Figures 2(b) and 3 show that, no matter what the shape of
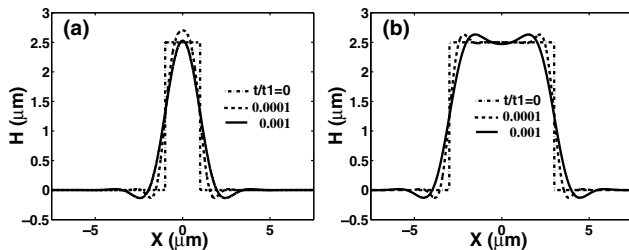
the topographic feature, QDs manage to align near the edges. It therefore cannot be simply the size of the substrate pattern that controls QD alignment.

A close inspection of all the images shows that the QDs nucleate in the most convex regions of the surface. As we discussed above, these regions have the highest chemical potential based on surface-energy considerations alone and, hence, ought to be the most unfavorable sites for 3D island nucleation and growth. On the other hand, the wetting layer of Ge ($\sim$ 3 ML) that forms in Ge hetero-epitaxy on Si is under compressive strain because of the 4% lattice mismatch between Ge and Si. The convex regions are most favorable for strain relaxation and therefore have the highest strain contribution to the chemical potential, which opposes the contribution from surface curvature. To determine the most favorable nucleation sites, we must determine the complete local chemical potential.

Microscopically, the effects of both surface curvature and strain can be understood in terms of atomic bonding. In a convex region, an atom has, on average, fewer neighbors, so its chemical-bond energy is smaller, increasing its chemical potential; however, its strain-relaxation energy is larger, as the compressed Ge atoms can stretch out more easily, decreasing its chemical potential. The reverse is true in a concave region. Thus, for a curved compressively strained film, the strain is partially relieved in the convex regions relative to a flat film, but enhanced in the concave regions. The degree of strain relaxation depends on local curvature.

To formulate the potential quantitatively, we assume the Ge wetting layer conforms exactly to the shape of the

FIG. 1. Simulated morphology evolution of (a) a stripe with 2 μm top width and (b) a square mesa (cross section) with 6 μm top width, under annealing at 1200 °C. t/t_1 is the normalized evolution time.
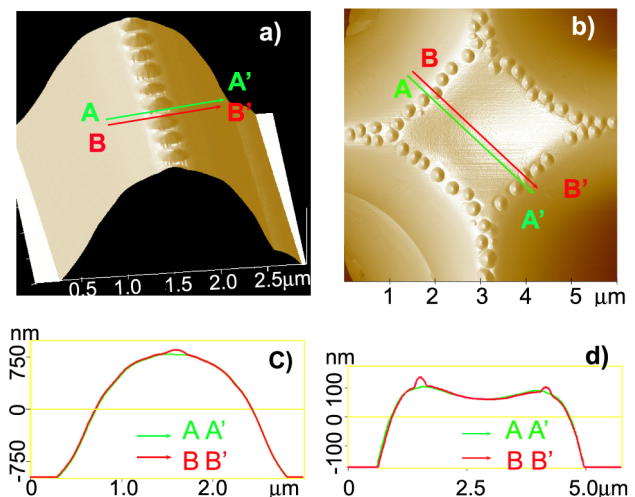

FIG. 2 (color online).   AFM images of Ge 3D island ordering on patterned Si(001) structures: (a) a stripe ridge; (b) a diamond-shaped stripe cross. (c) and (d) are the cross sections through (a) and (b), respectively, with AA' and BB' between dots and over dots, respectively. The z-scale difference in (c) and (d) is due to different plane-flatten processing. The nominal coverage is 60 ML.
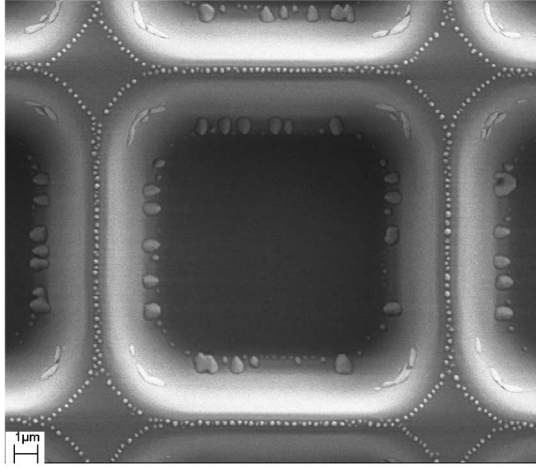
FIG. 3. Scanning electron microscope image of Ge 3D island ordering on patterned stripes on Si(001). $\theta_{Ge} = 60$ ML. The stripes are oriented in $\langle 110 \rangle$ directions, but ordering of Ge QDs is independent of direction. Other features (large islands at about half of the height in the upper corners, small islands at the bottom corners, etc.) can also be explained with the model [22].

FIG. 4. Variation of the local surface chemical potential of stripe structures with position X (solid line). The fitting parameter $(z_s - z_0)$ is 40 Å. The dashed line is the surface profile measured by AFM. The AFM scan underestimates the curvature because of tip convolution effects.

underlying patterned Si structures, and then we calculate the strain on the surface of the Ge film [$\epsilon(z_s)$] by treating it as a bent film [23], $\epsilon(z_s) = \kappa(z_s - z_0)$. κ is the local curvature, z_s is the position of the top surface, and z_0 is the position of the neutral plane of the bent film. The local strain-relaxation energy, relative to a flat film, is then

$$E_s = -\frac{C}{2}\left(\frac{\kappa}{|\kappa|}[\kappa(z_s - z_0)]^2 - \epsilon^2\right), \qquad (2)$$

where C is an elastic constant and ϵ is the misfit strain between the bent film and the substrate. The surface chemical potential of the film becomes

$$\mu = \mu_0 + \Omega\gamma\kappa + \Omega E_s, \qquad (3)$$

where the third term determines the strain contribution to the chemical potential. We use the AFM-generated [Fig. 2(a)] surface profiles (which will underestimate the curvature because of tip convolution effects) to calculate the locally varying surface chemical potential. The result is shown in Fig. 4. The dashed curve is the surface (height) profile obtained from AFM scans after standard spline curve fitting; the solid curve is the calculated surface chemical potential.

Figure 4 shows that the competition between the surface-energy and strain-energy terms leads to multiple local minima in the chemical potential. The surface-energy term (linear with surface curvature) produces chemical-potential minima in concave regions at the foot of stripes, and maxima in convex regions on the top ridges of stripes. The strain-relaxation term (quadratic in surface curvature) produces local chemical-potential minima in the most convex regions on the top ridges of stripes.
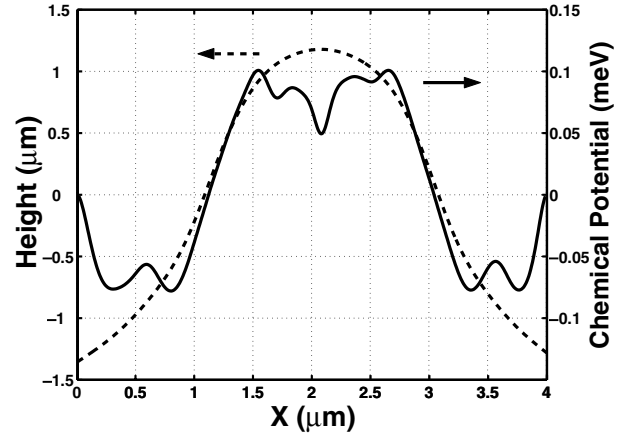
The positions of these calculated local chemical-potential minima agree very well with the observed locations of self-assembled Ge islands on the top ridges of stripes, as shown in Fig. 2(a). The local minima of chemical potential at the top ridge of the stripes are narrow and relatively deep, suggesting that the alignment and size uniformity of islands that form within these potential wells should be high. The creation of a narrow region of convex surface may play a key role in driving the self-assembled growth of strained islands, as these narrow convex regions provide a very localized strain relaxation. By tuning the surface curvature to modify the relative contributions of surface and strain energy, we can control the local surface chemical potential and thus the nucleation and alignment of Ge islands.

The concept of chemical-potential control of nucleation of QDs also applies qualitatively at the feet of stripes. As Fig. 3 shows, larger Ge crystals form along the feet of stripes, with less uniformity. The overall chemical potential is lower at the feet than on the tops of stripes, with a wider well and multiple minima. Thus large Ge crystals form with poor ordering and uniformity in these regions. Similar ideas apply at the regions of high curvature in the corners halfway up the stripes. They can be explained with a 3D version of our model, which will be discussed in detail elsewhere [22].

At the growth temperature, the chemical-potential variations in Fig. 4 are smaller than thermal energies of the diffusing species on the surface. However, thermal energies of adatoms do not have much influence on relative nucleation rates on the surface, whereas chemical potential changes do, and therefore even small changes of the chemical potential affect nucleation rates,

in accordance with the overall picture predicted by our model. At local chemical-potential minima on the surface, the adatom density is higher than in other places, and hence the probability of island nucleation is higher. In Fig. 4, the lowest chemical potential is at the feet of the ridges. Obviously, given enough time or high enough temperature, the dots forming on the ridges coarsen away, but these kinetics are slow.

The simple model we propose here explains previous puzzling observations of QD growth on patterned stripes and mesas. Several groups have reported that 3D islands tend to form in the valleys between patterned structures when no strained buffer layers (alloy films) are used, but, in contrast, form and order on the ridge (the top of the patterned structures) when strained buffer layers are deposited first [14,17]. One study [14] further shows that the thicker the strained buffer layer, the more the 3D islands tend to grow on the top ridges of patterns. These observations are completely consistent with our model. For patterned structures with submicron dimensions, the curvature contribution is generally large. When there is no strained buffer layer, the surface-energy term dominates the surface chemical potential, producing only a global minimum potential at the feet of the structures. The atoms diffuse toward this global minimum, and 3D islands nucleate at the feet of the structures. When a strained buffer layer is grown first, it adds the strain contribution to the surface chemical potential and introduces a potential minimum on the ridge top. Now 3D islands start to nucleate on the ridge. As the strained-buffer-layer thickness or the total strain in the strained buffer layer increases, the position of the neutral plane z_0 moves farther away from the surface z_s; hence $(z_s - z_0)$ increases. Because the strain component of the chemical potential increases quadratically with $(z_s - z_0)$ [Eq. (2)], the thicker the buffer layer or the larger the strain in the buffer layer, the larger the strain term, and the more likely 3D islands will form on the ridges. Using strained buffer layers of specific composition, it may therefore also be possible to control the size of QDs.

In conclusion, we present the concept of local strain-mediated chemical-potential control of self-assembly in heteroepitaxy. We demonstrate the self-assembly of Ge QDs on patterned Si(001) substrates using only simple photolithography and annealing. We achieve ordered growth of compact 1D arrays of QDs. Ge QDs prefer to nucleate and grow in the convex surface regions where local minima of surface chemical potential arise from the maximal strain relaxation of the wetting layer (or a strained buffer layer). The idea that the local chemical potential drives QD nucleation and growth explains prior results [14,17] and provides us with a unique method to control the self-assembly of islands by engineering patterned substrates with designed convex regions and designed buffer layers.

[1] S. Fafard *et al.*, Appl. Phys. Lett. **75**, 986 (1999).
[2] P. Schittenhelm *et al.*, J. Vac. Sci. Technol. B **16**, 1575 (1998).
[3] T. Lundstrom, W. Schoenfeld, H. Lee, and P. M. Petroff, Science **286**, 2312 (1999).
[4] S. Guha, A. Madhukar, and K. C. Rajkumar, Appl. Phys. Lett. **57**, 2110 (1990).
[5] D. J. Eaglesham and M. Cerullo, Phys. Rev. Lett. **64**, 1943 (1990).
[6] Y. W. Mo, D. E. Savage, B. S. Swartzentruber, and M. G. Lagally, Phys. Rev. Lett. **65**, 1020 (1990).
[7] F. Liu and M. G. Lagally, Surf. Sci. **386**, 169 (1997).
[8] A. W. Woll, P. Rugheimer, and M. G. Lagally, Mater. Sci. Eng. B **96**, 94 (2002).
[9] J. Drucker, IEEE J. Quantum Electron. **38**, 975 (2002).
[10] C. Teichert, J. C. Bean, and M. G. Lagally, Appl. Phys. A **67**, 675 (1998).
[11] T. I. Kamins and R. S. Williams, Appl. Phys. Lett. **71**, 1201 (1997).
[12] G. Jin *et al.*, Appl. Phys. Lett. **75**, 2752 (1999).
[13] L. Vescan, K. Grimm, and C. Dieker, J. Vac. Sci. Technol. B **16**, 1549 (1998).
[14] H. Lee *et al.*, Appl. Phys. Lett. **78**, 105 (2001).
[15] T. Kitajima, B. Liu, and S. R. Leone, Appl. Phys. Lett. **80**, 497 (2002).
[16] H. Omi, D. J. Bottomley, and T. Ogino, Appl. Phys. Lett. **80**, 1073 (2002).
[17] Z. Y. Zhong *et al.*, Appl. Phys. Lett. **82**, 445 (2003).
[18] W. M. Mullins, J. Appl. Phys. **28**, 333 (1957); **30**, 77 (1959).
[19] J. M. Blakely and H. Mykura, Acta Metall. **10**, 565 (1962); P. S. Maiya and J. M. Blakely, J. Appl. Phys. **38**, 698 (1967).
[20] C. Herring, in *Physics of Powder Metallurgy*, edited by W. E. Kingston (McGraw-Hill Inc., New York, 1951).
[21] Z. L. Liau and D. E. Mull, MIT Lincoln Laboratory Solid State Research Report No. 4, 1988.
[22] Bin Yang, Feng Liu, and M. G. Lagally (to be published).
[23] F. Liu *et al.*, Phys. Rev. Lett. **89**, 136101 (2002).